# Natural layer-by-layer photonic structure in the squamae of *Hoplia coerulea* (Coleoptera)

Jean Pol Vigneron,[1,*] Jean-François Colomer,[2] Nathalie Vigneron,[3,4] and Virginie Lousse[1,5]
[1]*Laboratoire de Physique du Solide, Facultés Universitaires Notre-Dame de la Paix, 61 rue de Bruxelles, B-5000 Namur, Belgium*
[2]*Laboratoire de résonance magnétique nucléaire, Facultés Universitaires Notre-Dame de la Paix, 61 rue de Bruxelles, B-5000 Namur, Belgium*
[3]*Ludwig Institute for Cancer Research, UCL 7459, Avenue Hippocrate 74, B-1200 Brussels, Belgium*
[4]*Section of Immunology, Yale School of Medicine, Yale University, New Haven, Connecticut 06520, USA*
[5]*Ginzton Laboratory, Stanford University, Stanford, California 94305, USA*
(Received 8 July 2005; published 12 December 2005)

The microscopic structure of the hard external parts of the body of the iridescent blue-violet chaffer beetle *Hoplia coerulea* is studied using scanning electron microscopy. The blue iridescence is shown to originate from the structure of the squamae within scales covering the dorsal side of the beetle. The internal structure of the scales shows a stack of planar sheets, separated by a well-organized network of spacers, a structure which belongs to the family of the layer-by-layer photonic crystals. The blue iridescence is easily explained by a planar multilayer approximation model, deduced from the observed three-dimensional structure.

DOI: 10.1103/PhysRevE.72.061904 PACS number(s): 42.66.−p, 42.70.Qs, 42.81.Qb

## I. INTRODUCTION

*Hoplia coerulea* (Coleoptera) belongs to the large family of *Scarabaeidae*. The blue hoplia can often be encountered from May to August, for instance, in the green vegetation bordering rivers and streams, in South European countries. The male displays a spectacular iridescent blue color, with violet large-angle reflections. The female is seldom seen, but its appearance is signaled by the gathering of a good number of blue iridescent males, more readily visible.

This paper deals with the origin of the colored reflectance from the male beetle's visible body surface. It has long been known that metallic coloration of birds and insects was often due to structural frequency selection, a fact which was already questioned in 1911 in a paper by Michelson [1]. The whole concept was revisited by Lord Rayleigh a few years later [2]. Structural colors are found in bird feathers [3], in butterfly wing scales [4–7] and many other biological surfaces [8,9], and organs [10,11]. These studies have recently been extended to the consideration of thermal exchanges [12] and ultraviolet protection [13].

The specific examination of beetles again dates back to Lord Rayleigh [14] and these studies already concluded in the structural origin of the iridescence for these insects. The case has been further studied in more recent years, with better microscopic tools [15] and on a much wider variety of species.

The consideration of *Hoplia coerulea* is interesting because, as will be shown in Fig. 1, it naturally realizes a layer-by-layer structure which, in principle, can easily be considered for synthesis with microfabrication techniques. Copying such a structure is still a challenge, however; the natural structure is designed to selectively reflect blue and violet radiation, an achievement which requires scaling down the photonic structure to reach a length scale of a few tens of nanometers.

This paper is organized as follows. Section II presents chosen scanning-electron micrographs of the scales of *Hoplia coerulea*, which describe the chitin structure found inside the iridescent squamae. Next, reflectance data are provided in Sec. III. These data are analyzed first in terms of a simple, planar multilayer model, in Sec. IV. This model is improved in Sec. V to assess the reflectance implied by the dielectric arrangement revealed by the microscopic investigation.

## II. SCANNING-ELECTRON MICROSCOPE IMAGES OF THE BEETLE CUTICLE

The cuticle, as seen in scanning-electron microscopy is shown in Fig. 2. The low-magnification image recorded on a Philips XL20 microscope (Namur) shows the head of the beetle, and part of its thorax. The body is covered by small, rounded scales, or squamae, attached by a single peripheral point to the underlying cuticle. These scales are easily removed by breaking this binding. Under an optical micro-


FIG. 1. (Color online) The male of the beetle *Hoplia coerulea* is conspicuous due to its iridescent blue-violet color. This coloration appears on most of the visible part of the exocuticle.

*Electronic address: jean-pol.vigneron@fundp.ac.be

 

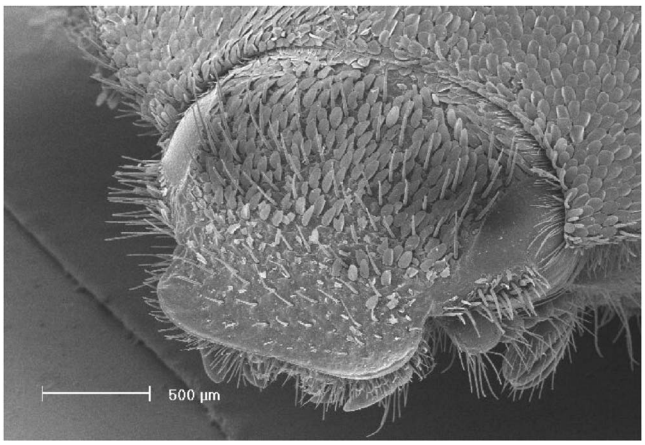


FIG. 2. The beetle's cuticle is, as seen here, covered by scales (squamae), often slightly curved out. The scales take the shape of a disk, with a diameter of about 50 $\mu$m and a thickness of 3.5 $\mu$m. The dorsal scales, seen under the optical microscope, render a blue or violet color.

scope, the dorsal scales are colored blue or violet-blue, while the ventral scales, as well as the scales on the legs, appear white, with a weak yellow-green iridescence. The samples used here were taken from dried specimens and prepared for observation in a scanning-electron microscope. In order to access the internal part of the scales, a piece of elytron was cooled down to liquid-nitrogen temperature (77 K) and a mechanical percussion was applied, all tools being kept in cryogenic conditions. Many scales were lost in this operation, but a proportion of the remaining ones were conveniently fractured and displayed part of their internal organization. A thin layer of gold (about 15 nm) was deposited on the sample before recording the images, as is usually done with insulating samples.

Figure 3 shows an enlarged view of the thickness of a fractured scale. These high-resolution pictures have been obtained on a JEOL JSM 5510 (Antwerp). The very flat envelope of the scales hides a structure which, at first sight, seems to be highly disordered. Similar images of the cross section of the scales have already been shown by Berthier [16]. From these and from the present work, it is clear that the squama structure is a stack of some 20 sheets parallel to the flat surface of the scale. Exploration of other remains gives a clearer view of the structure of these layers. Figure 4 shows a fragment of scale where the upper surface of one of the layers is clearly visible. The sheet is actually composed of a very thin plate of bulk chitin, bearing, on one side, a network of parallel rods with a roughly rectangular section.

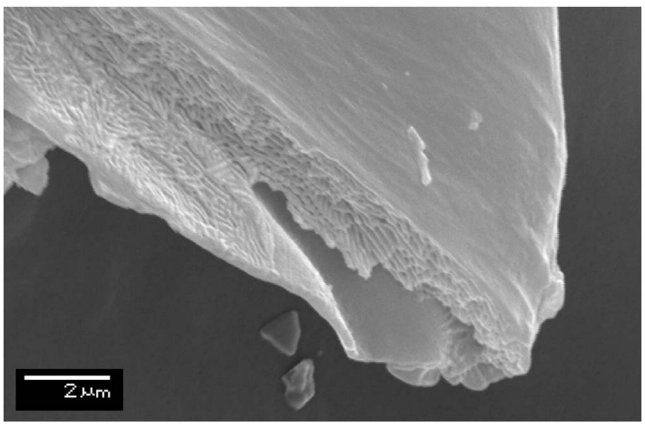


FIG. 3. Scale of the dorsal part of the hoplia body, fractured along a normal section. The flat cuticle which envelopes the scale hides a stack of chitin sheets. The sheets are well organized as layers, but no order of the sheet structure itself is revealed here. This figure indicates a scale thickness of about 3.4 $\mu$m, and a stack of about 22 sheets, i.e., a stack period of 160 nm.

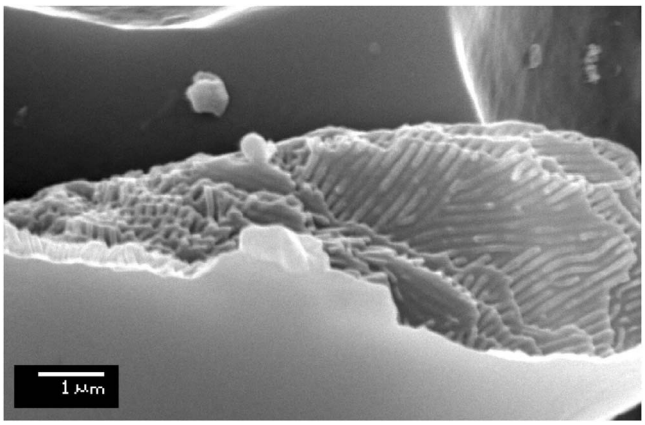


FIG. 4. Scanning-electron micrograph of a broken scale, revealing the structure of one of the sheets from the multilayer. The thin plate is covered by a network of parallel, equidistant rods. Locally, the structure is highly ordered, but the orientation of the rods looses some coherence over distances of the order of 5–10 rods spacings. The lateral period of the rods lattice can easily be estimated to be 170 nm.

These pictures give access to some geometric parameters which can be useful to elucidate the origin of the blue reflection produced by the scales. First, the thickness of the squamae is found to be of the order of 3.4 $\mu$m and the number of chitin sheets can be estimated to average 22. This leads to a stack period of 160 nm, which, as will be seen later, can explain the strong enhancement of a blue-violet reflectance. The structure of the sheets, revealed on the broken scale in Fig. 4, can also be quantified. In the lateral direction, the ridge network can be viewed as a set of parallel rods, with an axis-to-axis constant distance of 170 nm. The rods themselves have a cross-sectioned thickness of 115 nm, parallel to the sheet surface, leaving an air gap of 55 nm. The dimensions in the vertical direction are somewhat more difficult to access and we have to exploit the views provided by nonvertical fractures of the sheets, in Fig. 4 and similar images. The planar, base layer of each sheet is rather thin compared to the total 160-nm vertical period. It seems to occupy less than 25% of the total height, which means 40 nm. In some instances (see Fig. 5), this layer was thin enough to present local perforations. The material which constitutes these structured sheets is chitin, a biopolymer with refractive index close to 1.56 [11]. These data will be exploited in Secs. IV and V to build models to explain the color filtering function of this natural photonic device.

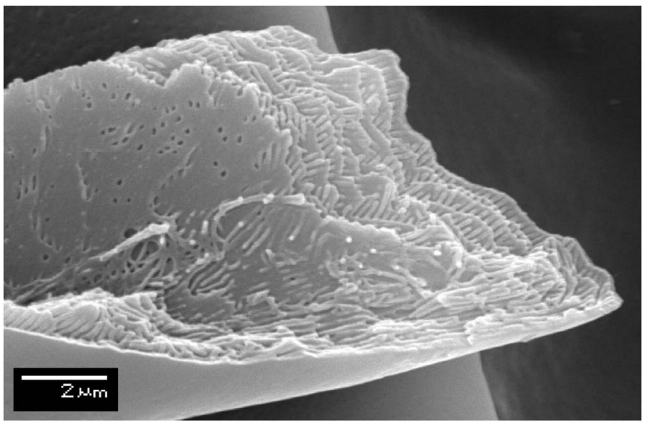


FIG. 5. This remain of the beetle scale shows the back side of the sheet stacked to form the biophotonic structure responsible for the *Hoplia* blue coloration. This back plate is in this case so thin that local perforations are apparent.

### III. REFLECTANCE SPECTRA

The dorsal reflection spectrum has first been investigated using an Avaspec 2048/2 fiber optic spectrometer. Measurements were performed, under a 30° incidence, in the specular direction. The reflected intensity is expressed in units of the corresponding diffuse reflection obtained on a standard white diffusor. The results are shown on Fig. 6. The strong reflection band extending between 380 nm and 480 nm explains the blue-violet iridescence observed on the dorsal side of the beetle. The rest of the visible spectrum is weakly reflected, which only very slightly desaturates the blue-violet hue of the insect.

### IV. PLANAR LAYERS MODEL

The strong blue-violet specular reflection can be understood on the basis of a very simple model. We consider a planar multilayer which alternates two slabs. The first one is

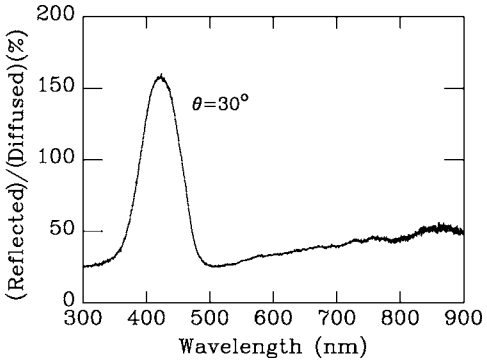


FIG. 6. Spectrum of light reflected from the elytrons (wing covers) of *Hoplia coerulea* in the specular direction. The strong reflection band extending between 380 nm and 480 nm explains the blue-violet coloration observed on the dorsal side of the beetle. The rest of the visible spectrum appears to be unstructured. The reflected intensity is compared to a white diffusely reflected intensity, not to the incident intensity.

the thin homogeneous back plate on which the network of rods is supported. This thin layer of chitin is given a thickness of 40 nm, with a refractive index of 1.56. The second homogeneous layer replaces the network of rods, with a thickness of 120 nm, to obtain a period of 160 nm, as observed.

The refractive index of this layer can be estimated in the following way. We assume near-normal incidence. According to the incident light polarization, the radiation electric field can be oriented along or across the ridges. When the field is oriented across the ridges, the average dielectric constant combines the chitin dielectric constant ($\varepsilon_1=2.43$) and the vacuum dielectric constant ($\varepsilon_2=1.00$) according to

$$\frac{\ell}{\varepsilon_\perp}=\frac{\ell_1}{\varepsilon_1}+\frac{\ell_2}{\varepsilon_2}, \tag{1}$$

where $\ell=170$ nm is the total transverse period of the rods array, split into $\ell_1=115$ nm of chitin, and $\ell_2=55$ nm of air. This gives $\varepsilon_\perp=1.66$. For a field oriented parallel to the ridges, the average dielectric constant verifies

$$\ell\varepsilon_\parallel=\ell_1\varepsilon_1+\ell_2\varepsilon_2 \tag{2}$$

and the dielectric constant turns out to be $\varepsilon_\parallel=1.97$. For unpolarized light, the average of these values turns out to be $\varepsilon=1.8$, a value which should be used for the homogenized layer containing the rods. A more elaborate model that avoids the homogenization step will be presented in Sec. V.

This simplified model provides much insight on the origin of the blue-violet coloration of the insect. In the case of a planar multilayer with low index contrasts, as is the case with chitin-based structures, one can easily predict the location of the frequency gaps which lead to the high-reflectance bands. At (or near) normal incidence, the gap in a multilayer of spatial period $a$ occurs at wavelengths such that the average-index light line meets the Brillouin zones boundaries of the one-dimensional periodic structure. These can be estimated as

$$\lambda=\frac{2a\bar{n}}{m}, \tag{3}$$

where $\bar{n}$ is the average refractive index in the period, and $m$ is an integer chosen so that the reflected wavelength $\lambda$ lies in the spectral interval of interest (here, the narrow interval which corresponds to the visible range). With a period $a=160$ nm and an average refractive index $\bar{n}=1.4$, we get, for $m=1$, $\lambda=448$ nm. Clearly, this simple formula easily succeeds to predict the blue iridescence observed, confirming that, at least near normal incidence, the structure discovered in the insect squamae can be viewed as a planar multilayer selective reflector. In order to obtain the required contrast, and using a single biopolymeric material, the insect has laterally structured one of the layers in the period, introducing just enough air to provide a contrast which opens up the reflective stop band prepared for the blue-violet region.

The above simplified model succeeds in explaining the near-normal reflectance dominant wavelength, but the observed spectral profile shown in Fig. 7 is not so well described, and this should be given some justification. A planar

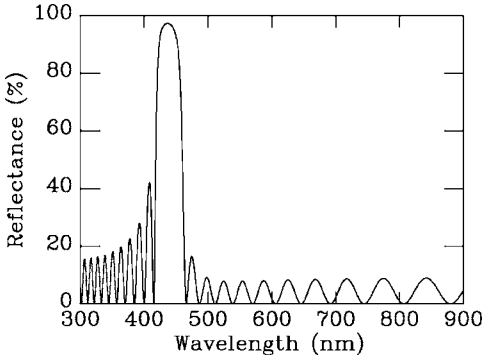


FIG. 7. Calculated reflectance spectrum of the planar multilayer model for *Hoplia coerulea* scale internal structure. In this model, the corrugated layer is replaced by an homogeneous plate of average refractive index 1.34 ($\varepsilon=1.8$).

multilayer stop-band reflection usually presents a rounded square-top spectral profile, not recognized in the triangular line shown in Fig. 6. The line-shape transformation can be attributed to the irregularities in the geometry of the squamae, which, as implanted, show some orientation disorder. The angular uncertainty can be roughly estimated from the scanning-electron microscope images to be in the order of 30°. Figure 8 shows the result of averaging the reflectance spectra over the incidence angles for a centered angular window. The averaging process approximately realizes the convolution of the central incidence spectrum with a square-top angular window, which naturally leads to the triangular line shape seen in the experiment. Figure 8 also shows the shift of the dominant wavelength from blue to violet when the angle of incidence is increased. This color change is seen as a blue-violet iridescence when the insect is exposed to daylight.

Further simulations show that the width of the averaged triangular line is not very sensitive to the choice of the disorientation angular window. The slight discrepancy which remains between the measured and modeled spectral profile cannot be accounted for by assuming uncertainties on this parameter. A more convincing explanation lies in the fact that the stack of layers shows structural disorder. This disorder can be thought of as a random change of refractive index and layer thickness from one corrugated layer to the next, a change which randomly modifies the optical path and the resonance frequency in each of the 20–25 periods stacked in the insect scales. Figure 9 shows the effect of such a disorder ($\pm 10\%$) applied to the average dielectric constant, and to the layer thickness. The simulation shows that the observed spectral band shape can also be approached in the framework of a model reduced to one dimension.

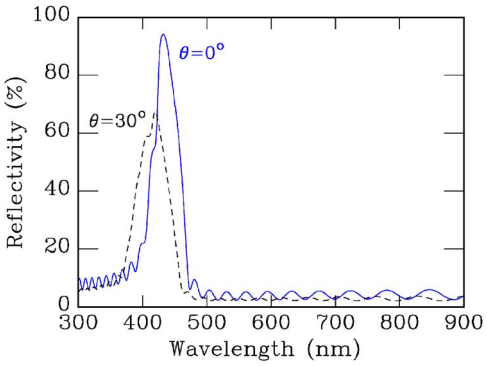


FIG. 8. (Color online) Calculated specular reflectance spectrum of the one-dimensional averaged model. The reflectivity is averaged over the incident angles $\theta$ in an angular window 30° wide. The reflectivity is modeled for two central incidences, $\theta=0°\pm15°$ and $\theta=30°\pm15°$.

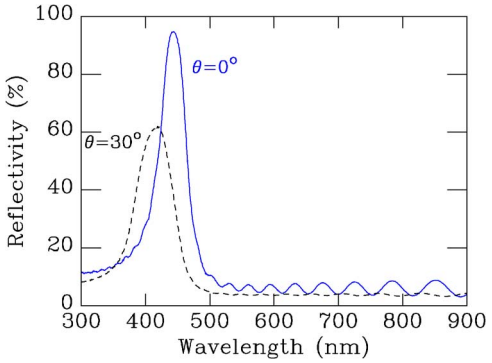


FIG. 9. (Color online) Calculated specular reflectance spectrum of the one-dimensional averaged model, with 10% disorder in the corrugated layer. As in Fig. 8, the reflectivity is averaged over the incident angles $\theta$ in an angular window 30° wide. The reflectivity is modeled for two central incidences, $\theta=0°\pm15°$ and $\theta=30°\pm15°$.

## V. NOTE ON THREE-DIMENSIONAL CONTRIBUTIONS

The above one-dimensional model provides a clear understanding of the reflectance spectrum, though all three-dimensional details have been averaged out. In this section, we specifically look for three-dimensional effects, which would provide information on the way the corrugated layers are arranged or related to each other. One such property is anisotropy, which could show up if the rod network in the different layers tends to take a common orientation. This could be the case, if the growing mechanism of the scale puts a strong constraint on the rods geometry.

An extreme case, which most probably exaggerates anisotropy, assumes that the rods are all oriented in a longitudinal direction, parallel to the symmetry plane of the animal. Using three-dimensional $S$ transfer-matrices [17], the dominant wavelength is calculated and displayed in Fig. 10 as a function of two angles: (1) the incidence angle $\theta$ (angle between the incident wave and the normal to the scale surface), and (2) the azimuthal angle $\phi$, counted here from the perpendicular to the rods, at right angle with the symmetry plane of the animal. $\phi=0°$ and $\phi=180°$, refer to the direction perpendicular to the rods, viewing the animal from the side; $\phi=90°$ is an observation direction along the rods, parallel to the animal symmetry plane.

The left panel on Fig. 10 (negative azimuthal angles) is the three-dimensional map, accounting for azimuthal anisotropy, while the right panel (positive azimuthal angles) shows the same information, calculated with the homogenized one-dimensional stack model. In wide regions, the

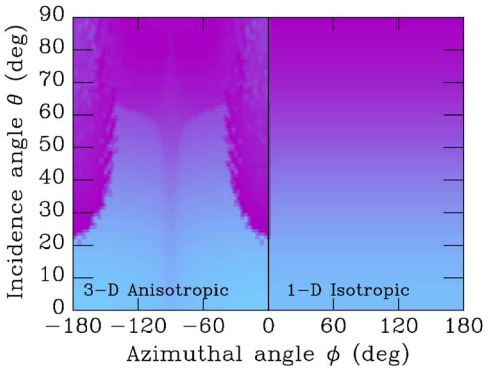


FIG. 10. (Color online) Calculated dominant reflected wavelength (light tone is blue, dark tone is violet), accounting for anisotropy (negative $\phi$) and neglecting anisotropy (positive $\phi$). The incidence angle $\theta$ is measured from the normal to the squama surface, and the azimuthal angle $\phi$ is measured from the normal to the symmetry plane of the animal, assuming the rods are roughly oriented along this symmetry plane.

simple one-dimensional model agrees well with the three-dimensional calculation. But we note a significant difference: if the rod orientation was correlated, the violet color would occur abruptly at small (20°) increasing incidence angles when viewing the animal from the side ($\phi$=0°). Then, the iridescence would be somewhat easier to detect in the transverse direction than in the longitudinal direction. This subtle effect is not easily confirmed by observations of the insect with the unaided eye nor, indeed, by careful measurements. Figure 11 shows the specular reflectance, measured on the back of the insect, for increasing incidence angles $\theta$, in the transverse ($\phi$=0°) and longitudinal ($\phi$=90°) directions. The contrast between these two cases has clearly no significance, so that anisotropy of the internal scale structure is not clearly detectable. Consistent with the indications given by images such as that in Fig. 6, the layer-by-layer stack in the scales contains enough orientation disorder to avoid the manifestation of three-dimensional coherence effects.

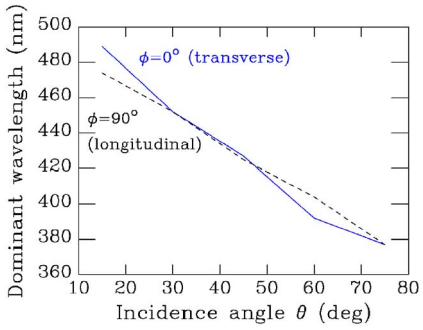


FIG. 11. (Color online) Measured dominant wavelength for various angles of incidence $\theta$ for two azimuthal orientations. When $\phi$=90°, the incidence plane is the insect vertical left-right symmetry plane, oriented in the longitudinal direction, from tail to head. When $\phi$=0°, the incidence plane is in the transverse direction, crossing the elytrons perpendicular to the symmetry plane.

## VI. CONCLUSION

The coleoptera *Hoplia coerulea*, male, shows a vivid blue coloration which originates from the structure of the squamae within the scales covering the observable part of its exocuticle. Investigation of the structure of these squamae reveals that these cuticular scales are photonic devices involving a layer-by-layer structure: alternating thin plates with rows of parallel rods.

This structure gives rise to a high-reflection band in the blue part of the visible spectrum, which shifts to the violet as the incidence angle is increased. This reflection is caused by interferences in the layer-by-layer structure, which presents a stop-band (incomplete photonic gap) at wavelengths close to 450 nm, under normal incidence. Most of the quantitative aspects of the coloration process can be accounted for by a one-dimensional model involving only isotropic materials. In this model, the dielectric constant of the network of rods is represented by a carefully averaged value. This one-dimensional stack model correctly suggests the change of color from blue to violet when the angle of incidence is increased from near normal to grazing the scale surface. However, we note that the detailed spectral profile of the reflection band is only understood if we account for disorder at two different length scales: on one hand, the disorder in the orientation of the squamae within the scales and, on the other hand, the disorder in the internal structure of the squamae. Both seem necessary to produce the triangular shape of the reflection band. No specific three-dimensional, diffractive pattern behavior was observed, so that the lateral structuring of the layers is best considered as a means of producing a carefully engineered refractive index variation within a mixture of air and chitin.

The cyano-blue coloration of this insect is quite exceptional and it would be most interesting to know whether this selective reflectance of the male has actually provided any understandable advantage which helped the species to keep a significant population over time. Very likely, the blue-violet iridescence can serve conspecific recognition. However, assessing the real importance of this precise factor in front of the many other links of this insect to its environment is a very complex work, obviously far beyond the scope of the present physical analysis.

## ACKNOWLEDGMENTS

The authors thank Professor Amand Lucas for a helpful critical reading and Professor Van Tendeloo for his invitation to use the JEOL JSM 5510 of the EMAT Center (University of Antwerp). The help of Louise Samain, Annick Bay, Benjamin Bera, and Ivan Ducarme, freshman students at the University of Namur, Belgium, is gratefully acknowledged. This work was carried out with support from EU5 Centre of Excellence ICAI-CT-2000-70029 and from the Inter-University Attraction Pole (IUAP P5/1) on Quantum-size effects in nanostructured materials of the Belgian Office for Scientific, Technical, and Cultural Affairs. The authors acknowledge the use of Namur Interuniversity Scientific Computing

Facility (Namur-ISCF), a common project between the Belgian National Fund for Scientific Research (FNRS), and the Facultés Universitaires Notre-Dame de la Paix (FUNDP). This work has also been partly supported by the European Regional Development Fund (ERDF) and the Walloon Regional Government under the "PREMIO" INTERREG IIIa project. V.L. and J.F.C. were supported by the Belgian National Fund for Scientific Research (FNRS).

[1] A. A. Michelson, Philos. Mag. **21**, 554 (1911).
[2] Lord Rayleigh, O. M., F. R. S., Philos. Mag. **37**, 98 (1918).
[3] C. W. Mason, J. Phys. Chem. **27**, 210 (1923).
[4] K. Gentil, Z. Morphol. Oekol. Tiere **38**, 344 (1942).
[5] R. L. Taylor, Entomol. News **75**, 253 (1964).
[6] P. Vukusic, J. Sambles, C. Lawrence, and R. Wootton, Proc. R. Soc. London **266**, 1403 (1999).
[7] B. Gralak, G. Tayeb, and S. Enoch, Opt. Express **9**, 567 (2001).
[8] C. G. Bernhard, G. Gemne, and A. R. Moeller, Q. Rev. Biophys. **1**, 89 (1968).
[9] C. W. Mason, J. Phys. Chem. **31**, 321 (1927).
[10] Y. P. Nekrutenko, Nature (London) **205**, 417 (1965).
[11] A. R. Parker, R. C. McPhedran, D. R. McKenzie, L. C. Botten, and N. A. Nicorovici, Nature **409**, 36 (2001).
[12] L. P. Biró, Z. Bálint, K. Kertész, Z. Vértesy, G. I. Márk, Z. E. Horváth, J. Balázs, D. Méhn, I. Kiricsi, V. Lousse, and J.-P. Vigneron, Phys. Rev. E **67**, 021907 (2003).
[13] J. P. Vigneron, M. Rassart, Z. Vértesy, K. Kertész, M. Sarrazin, L. P. Biró, D. Ertz, and V. Lousse, Phys. Rev. E **71**, 011906 (2005).
[14] Lord Rayleigh, O. M., F. R. S., Proc. R. Soc. London **103**, 233 (1923).
[15] A. C. Neville and S. Caveney, Biol. Rev. Cambridge Philos. Soc. **44**, 531 (1969).
[16] S. Berthier, *Iridescences, les Couleurs Physiques des Insectes* (Springer-Verlag, Paris, 2003).
[17] J. B. Pendry and A. MacKinnon, Phys. Rev. Lett. **69**, 2772 (1992).